Abstract—A new description of growth in blacklip abalone (*Haliotis rubra*) with the use of an inverse-logistic model is introduced. The inverse-logistic model avoids the disadvantageous assumptions of either rapid or slow growth for small and juvenile individuals implied by the von Bertalanffy and Gompertz growth models, respectively, and allows for indeterminate growth where necessary. An inverse-logistic model was used to estimate the expected mean growth increment for different blacklip abalone populations around southern Tasmania, Australia. Estimates of the time needed for abalone to grow from settlement until recruitment (at 138 mm shell length) into the fishery varied from eight to nine years. The variability of the residuals about the predicted mean growth increments was described with either a second inverse-logistic relationship (standard deviation vs. initial length) or by a power relationship (standard deviation vs. predicted growth increment). The inverse-logistic model can describe linear growth of small and juvenile abalone (as observed in Tasmania), as well as a spectrum of growth possibilities, from determinate to indeterminate growth (a spectrum that would lead to a spread of maximum lengths).

Using an inverse-logistic model to describe growth increments of blacklip abalone (*Haliotis rubra*) in Tasmania

Malcolm Haddon (contact author)

Craig Mundy

David Tarbath

Email address for M. Haddon: Malcolm.Haddon@utas.edu.au

Marine Research Laboratory
Tasmanian Aquaculture and Fisheries Institute
University of Tasmania
Nubeena Crescent
Taroona TAS 7051, Tasmania, Australia

Blacklip abalone (*Haliotis rubra*) constitute the most valuable fishery in Tasmania, Australia, yielding approximately 30% (2500 tonnes) of the resource captured in the wild worldwide, worth more than AU$100 million per year. There are significant difficulties in determining the age of blacklip abalone (McShane and Smith, 1992), making them good candidates for size-structured assessment modeling (Sullivan et al, 1990; Punt and Kennedy, 1997). Although used informally in the Tasmanian fishery, size-structured models are used formally to assess blacklip abalone stocks elsewhere in Australia (Worthington et al., 1998; Gorfine et al., 2005) and to assess Paua (*H. iris*) in New Zealand (Breen et al., 2003). With size-structured models it is important to generate a precise and unbiased mathematical description of growth because the adoption of an inappropriate growth model could have significant effects on the outcome of an assessment.

Day and Fleming (1992) reviewed a range of models previously used to describe abalone growth. In total, 59 growth studies have been undertaken on different abalone species. The von Bertalanffy growth curve (von Bertalanffy, 1938) has been used in 42 (71%) of these studies and the Gompertz model (Gompertz, 1825). has been used in four studies (6.78%). The dominance of the von Bertalanffy growth model reflects its almost universal adoption in abalone fisheries

assessments and the relative ease with which it can be fitted to growth data taken from tagging experiments (Fabens, 1965; Francis, 1988; Haddon, 2001). In nine studies (15.25%), linear growth was proposed, but the focus of these nine studies was on juvenile and small abalone and that focus could imply that growth alters its character above a particular size, at least in some species. A flexible growth description has also been given by Francis (1995) who generated a size-based analogue to the age-based growth description by Schnute (1981). Francis's model has been used in New South Wales, Australia (Worthington et al., 1998), and New Zealand assessments of abalone (Breen et al., 2003).

Sainsbury (1982a, 1982b) fitted von Bertalanffy growth curves to abalone tagging data from New Zealand (*H. iris*). Instead of assuming that the familiar parameters (L_∞, the asymptotic maximum size, and K, the growth coefficient in the von Bertalanffy equation) were averages for the population, Sainsbury (1982a) inferred the growth dynamics implied when each individual had its own set of von Bertalanffy parameters. Essentially, the growth characteristics of individuals were assumed to be variable and were described by using probability density functions to represent the model parameters. Similarly, a probability density function form of the Gompertz growth model was used in Victoria, Australia (Troynikov and

Table 1

Data by sites and regional groupings of sites (Fig. 1) in southern Tasmania where blacklip abalone (*Haliotis rubra*) were collected to compare growth rates. Time step relates to whether the analysis was for annual or seasonal growth, count is the number of tags recovered, and Min–Max Init. *L* (in mm) are the minimum and maximum initial length of blacklip abalone at tagging for each site.

Time step	Longitude (East)	Latitude (South)	Regional grouping	Site name	Count n	Min–Max Init. L
Annual	145.492	−42.969	Southwest	Black Island	116	57–171
Annual	145.667	−43.075	Southwest	Giblin River	84	83–173
Annual	145.781	−43.226	Southwest	Hobbs Island	57	57–181
Annual	146.900	−43.566	Actaeon	Gagens Point	154	50–142
Annual	146.972	−43.549	Actaeon	Middle Ground	353	47–146
Annual	147.381	−43.366	Bruny Island	Fluted Cape	135	83–154
Annual	147.385	−43.111	Bruny Island	One Tree Point	162	52–153
Seasonal	146.996	−43.534	Actaeon	Actaeon Island	390	61–176
Seasonal	146.990	−43.550	Actaeon	Sterile Island	373	48–146

Gorfine, 1998; Troynikov et al., 1998; Bardos, 2005). Like the von Bertalanffy model, the Gompertz equation is deterministic in predicting an asymptotic maximum length. The probabilistic forms of these two models predict a more plausible range of final maximum lengths and some configurations of Francis's (1995) model can also exhibit a spread of final sizes. However, like the von Bertalanffy and Gompertz models, Francis's (1995) model fails to exhibit the linear-like early growth of small abalone that has been observed in Tasmania.

An important characteristic of growth models is an ability to accurately model growth across a broad size range. Nine of the studies cited in Day and Fleming (1992) indicate that early growth in abalone is effectively linear. This linearity contrasts strongly with both the von Bertalanffy curve (which predicts faster early growth) and the Gompertz growth curve (which predicts slower early growth). Neither the von Bertalanffy nor the Gompertz growth models are consistent with observations of effectively linear growth in small blacklip abalone in Tasmania, Australia (Prince et al., 1988; Gurney et al., 2005). Such early linear-like growth would imply constant growth increments in small animals and would require a different structural model to represent such growth dynamics.

Given the wide variation in maximum sizes found in natural abalone populations, an alternative approach to using deterministic models (with a known or even probabilistic asymptotic length) would be to model growth as indeterminate. Indeterminate growth would imply no specific upper limit and animals would be expected to continue growing, even if very slowly, until they die. This indeterminacy would have the disadvantage in that there would be no simple analytical solution for length-at-age, but nevertheless this strategy could provide for intuitively simple empirical descriptions of growth that avoid the complexities of fitting probabilistic models as proposed by Sainsbury (1982a) and Bardos (2005).

Here we present a new empirical description of blacklip abalone growth using an inverse-logistic model for both the mean growth increment and the predicted variation about the mean increment for a given shell length. In contrast to both the von Bertalanffy and Gompertz growth curves, the growth description given here allows for both linear growth of small and juvenile abalone as well as the option of either determinate growth (with a maximum shell length) or indeterminate growth (with a spread of maximum lengths).

Materials and methods

Examination of growth patterns

To provide an initial empirical indication of growth patterns, the size of abalone at tagging were grouped into 10-mm classes and the mean growth increment in each class was then plotted on top of the raw data from the southwest area of Tasmania (a combination of three sites, Fig. 1; Table 1).

Tagging methods and locations

Two sets of data were used in the description of the inverse-logistic model. Firstly, to examine annual growth increments, we used tagging data from seven sites around the south of Tasmania (Fig. 1). Data from those sites were limited to tagged-and-recaptured abalone and the data were collected approximately one year apart (between 0.96 and 1.05 years apart). Abalone from some groups of sites were found to exhibit very similar growth patterns and the data from these sites were combined to generate three larger regions (namely, southwest, Actaeon, and Bruny Island) (Fig. 1; Table 1). Secondly, tagging data from two sites were used to examine seasonal growth (Table 1), and for this analysis,
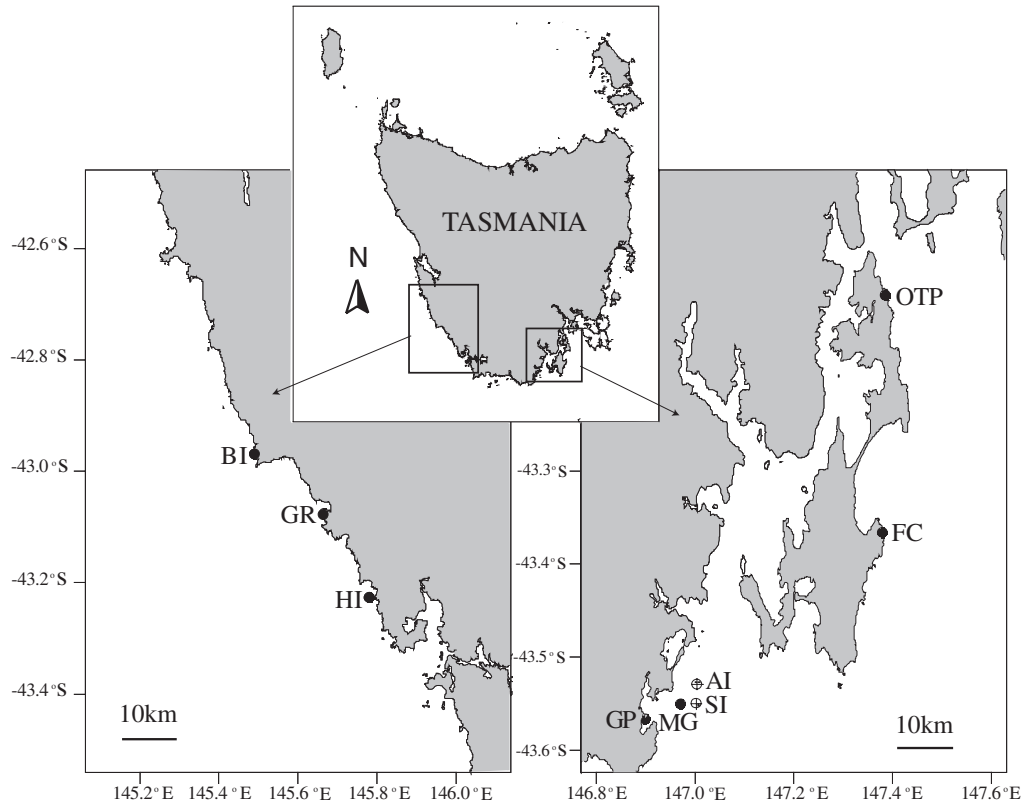
Figure 1

A map of Tasmania indicating the locations (black dots) from which the data on blacklip abalone (*Haliotis rubra*) growth increment patterns were collected. Left panel represents the southwest region comprising three sites: BI=Black Island, GR=Giblin River, and HI=Hobbs Island. Right panel represents the Actaeon region (comprising two sites: the GP=Gagens Point and MG=Middle Ground sites) and the Bruny Island region (comprising two sites: FC=Fluted Cape and OTP=One Tree Point sites). Seasonal data are identified by a combination of a circle and cross for both the Actaeon Island (AI) and Sterile Island (SI) sites (Table 1).

tagging and recaptures were scattered throughout the year and the recapture intervals ranged from 0.06 to 1.99 years.

We tagged blacklip abalone by inserting a plastic rivet into the open exhalent hole furthest from the shell lip. The rate of tag fouling, and the increased risk of the tag not being found, increased dramatically after two years; therefore, only tags at liberty for less than two years were used in the analyses of seasonal growth. Across all sites, tagged abalone ranged in size from 47 mm to 181 mm shell length, but ranges varied at each site (Table 1). Measurements of maximum shell length were taken to the nearest 1.0 mm.

There is some evidence that tagging can negatively affect the growth of tagged animals, producing a tagging shock in affected individuals (Prince et al., 1988). It seems plausible that at least some of the variability in growth observed in abalone tagging experiments derived from different responses to the tagging process. In an attempt to minimize such effects in this study, tagging methods were standardized; animals were kept damp and cool during the tagging process before being returned to their reefs by divers. Blacklip abalone <50 mm shell length were not sampled because they tend to be highly cryptic in Tasmania, initial capture below this size is difficult, and adhesives rather than rivets, must be used to attach tags to young abalone.

Growth model

The units of growth used here are the growth increments (ΔL) produced by animals of known starting lengths (L_t) that have been at liberty for varying lengths of time (Δt). The model structure includes seasonality by default, and the seasonality terms are set to have zero influence to form an annual model. The form of the inverse-logistic curve used is a typical logistic selectivity curve described by Haddon (2001).

Growth of blacklip abalone does not differ between the sexes. An inverse-logistic model was used to describe the expected length increment ΔL for a known initial size L_t:

$$\Delta L = \frac{Max\Delta L \times \begin{bmatrix} \Delta t + C\sin\left(2\pi\left(t_R - p\right)\right) - \\ C\sin\left(2\pi\left(t_T - p\right)\right) \end{bmatrix}}{1 + e^{Ln(19)\frac{\left(L_t - L_{50}^m\right)}{\left(L_{95}^m - L_{50}^m\right)}}} + \varepsilon_{L_t}, \qquad (1)$$

where $Max\Delta L$ = the hypothetical asymptotic maximum growth increment at some initial size of abalone that sets the exponential term to zero;

Δt = the interval between tagging and recapture (as a fraction of a year);

L_t = the size when first tagged;

L_{50}^m = the initial length at which the midway point between the $Max\Delta L$ and lowest growth increment is reached;

L_{95}^m = the initial length at which 95% of the difference between the smallest and maximum increment is reached;

C = the amplitude of the seasonality effect for ΔL;

t_R and t_T = the dates of recapture and tagging, respectively (as fractions of a year, e.g., June 30th = 0.5; $t_R = t_T + \Delta t$); and

p = the date of maximum growth rate (as a fraction of a year).

The error term ε_{L_t} is additive and normal, and is assumed to have a mean of zero and standard deviation σ_{L_t} that can be defined either as a function of initial length, L_t, or as a function of the predicted length increment $\Delta\hat{L}_t$. If the expected length increments ever attain zero, or go negative, then the standard deviation of the residuals σ_{L_t} can be defined in terms of the initial length L_t:

$$\sigma_{L_t} = \frac{Max\sigma_L \times \begin{bmatrix} \Delta t + C_\sigma\sin\left(2\pi\left(t_R - p\right)\right) - \\ C_\sigma\sin\left(2\pi\left(t_T - p\right)\right) \end{bmatrix}}{1 + e^{Ln(19)\frac{L_t - L_{50}^s}{L_{95}^s - L_{50}^s}}}, \qquad (2)$$

where $Max\sigma_L$ = the hypothetical asymptotic maximum standard deviation of the residual values at some initial size of abalone that sets the exponential term to zero;

L_{50}^S and L_{95}^S = the parameters describing the inverse-logistic for how the variability of residuals reduces with increasing L_t; and

C_σ = the amplitude of the seasonality effect for the σ_{L_t} term.

The fact that $Ln(19)$ is used instead of $-Ln(19)$ implies that the logistic is inverse and that the L_{95} parameters relates to the 95% point ($Ln(15)$ would equate to the 75% point). The inverse-logistic description of variation is general; however, if the expected length increments always remain greater than zero then the standard deviation of the residuals σ_{L_t} can be defined as the simpler

$$\sigma_{L_t} = \alpha\left(\Delta\hat{L}_t\right)^\beta, \qquad (3)$$

where α and β are parameters of a power relationship with the expected length increment $\Delta\hat{L}_t$ and the seasonality is achieved from Equation 1.

When seasonality is ignored (when estimating annual growth increments), the C and C_σ parameters are set to zero leaving the simple Δt so that any slight deviations from a Δt of one year are assumed to alter the predicted growth in a linear fashion. Thus, 0.95 of a year permits 95% of the growth increment of that year. With the use of Δt alone, there is the assumption that a simple linear scaling of growth increment with respect to time elapsed will provide sufficient adjustment for small deviations of Δt from one year.

Using a normal distribution to describe the residuals, we found that there was an excellent match of this distribution to available data. However, if some probability density function other than the normal distribution provided a better fit for some other species or population, then the equivalent measure of spread about the expectation would need to be implemented.

Where the tagging interval is greater than one year, the expected growth increment is estimated in two steps. First, the expected growth increment and standard deviation that would be expected during **a** year of growth are estimated, and then the growth increment for the fraction of the year remaining from the date of tagging to the date of recapture (after subtracting one year) is estimated by using the initial size plus the estimated yearly growth increment as the starting length for the second installment of growth. Thus, ΔL is first estimated with Equation 1 with the C and C_σ parameters set to zero, and Δt set to 1.0, and then the fraction of a year remaining from the date of tagging to the date of recapture (after subtracting one year) is used in the full version of Equation 1 and the L_t is set to the original L_t plus the ΔL predicted from one year of growth. The two sequential ΔL estimates are added together to obtain the total predicted growth increment. Using Equation 2 to define the variation about the curve, we applied a similar sequential process to the estimation of the standard deviation of the respective residual errors. In this case, the expectation was that the variability would reduce with increasing size so the C_σ parameter was expected to be negative rather than positive as was expected for the C parameter. The use of Equation 3 requires that it be applied to

the predicted ΔL. Given that the first year of growth is always assumed to equal the average increment, there is an increased chance that the overall variability of the residuals will be underestimated. However, in practice, bias appears to be small as long as the data available from greater than a single year overlap the available data from durations less than a year in terms of the initial shell lengths.

Alternative growth models

To provide a comparison with the inverse-logistic model both the von Bertalanffy (Fabens, 1965) and Gompertz curves (Troynikov et al., 1998) were fitted to the tagging increment data from southwest Tasmania:

$$\Delta L = \left(L_\infty - L_t\right)\left(1 - e^{-K\Delta t}\right), \tag{4}$$

where L_∞ = the asymptotic maximum size; and
K = the von Bertalanffy growth rate coefficient; and

with

$$\Delta L = L_\infty \left(\frac{L_t}{L_\infty}\right)^{\exp(-g\Delta t)} - L_t, \tag{5}$$

where g = the growth rate parameter in the Gompertz equation.

Likelihoods

At each geographical site, normal likelihoods with non-constant variances (Eqs. 2 or 3), were used to fit the inverse-logistic model to the n available data points. The negative log-likelihood was minimized to determine the optimum parameter estimates:

$$-veLL = -\sum_{L_t=1}^{n} Ln\left[\frac{1}{\sqrt{2\pi}\sigma_{L_t}}e^{\frac{-\left[\left(\Delta L - \Delta \hat{L}\right)^2\right]}{2\sigma_{L_t}^2}}\right]. \tag{6}$$

The nonlinear solver in Excel 2003™ (Microsoft, Seattle, WA) was used to fit all models.

Alternative model arrangements

The full seasonal model has nine parameters, but alternative model structures are possible that use fewer parameters. The alternative model structures suggested relate to the description of the variability about the expected curve. With the seasonal growth description, instead of using Equation 2 to describe the expected residual structure with the Tasmanian data, an acceptable alternative was to ignore the denominator and focus only on the seasonal changes in variability, thus reducing the number of parameters to seven:

$$\sigma_{L_t} = Max\sigma_L \times \left[\begin{array}{c}\Delta_t + C_\sigma \sin\left(2\pi\left(t_R - p\right)\right) - \\ C_\sigma \sin\left(2\pi\left(t_T - p\right)\right)\end{array}\right]. \tag{7}$$

An alternative approach to implementing this structural change would be to set the L_{50}^S and L_{95}^S parameters in the denominator of Equation 2 to values much larger than the maximum observed initial size. This change in the denominator leads to the exponential term becoming insignificant so that the denominator contracts to one, the division thus has no noticeable effect, and Equation 2 becomes equivalent to Equation 7.

When only annual data are available, the seasonality terms could be ignored and thus a six-parameter model could be used. After the six-parameter model was fitted to real data, it became clear that the L_{95}^S value was often close to the maximum size of abalone found in Tasmania; therefore it was possible to generate a five-parameter model by replacing the L_{95}^S parameter with a constant 210 mm (the size of an abalone that was never tagged but sometimes found in nature). In addition, the L_{50}^S value was often close to the L_{95}^m value. By replacing the former with the latter it was possible to generate a four-parameter model:

$$\sigma_{L_t} = \frac{Max\sigma_L \times \Delta t}{1 + e^{Ln(19)\frac{L_t - L_{95}^m}{210 - L_{95}^m}}}. \tag{8}$$

The three alternative annual models (4, 5, and 6-parameter models) were fitted to the available data from the three regional groups of sites from around southern Tasmania. A comparison of the relative fit of each model was made by using Akaike's information criterion, $AIC = -2LL + 2k$, where LL is the log-likelihood and k is the number of parameters. In addition, the Bayesian Information Criterion $BIC = -2LL + kLn(n)$ was also used, where n is the total number of observations (Burnham and Anderson, 2002). For each of these statistics, the model with the smallest value is to be preferred (Quinn and Deriso, 1999). The AIC only includes the log-likelihood and the number of parameters, whereas the BIC also includes the natural log of the sample size. Where the sample size is greater than 7 [Ln(7.389)=2], the BIC penalizes the addition of extra parameters more than the AIC. Thus, with the sample sizes observed in the tagging data (Table 1) the BIC would be expected to recommend more parsimonious models (those with fewer parameters) than would the AIC.

In addition to comparing the AIC and BIC values for the different models, likelihood ratio tests were conducted to compare the alternative model fits by using different numbers of parameters (Quinn and Deriso, 1999; Haddon, 2001). Given the log-likelihood for each model fit, the likelihood ratio test is

$$\chi^2_{df} = -2(LL_R - LL_F), \qquad (9)$$

where LL_R = the log-likelihood for the model with fewest parameters; and

LL_F = the log-likelihood of the model with most parameters.

In the chi-squared statistic, χ^2_{df}, df is the difference in number of parameters (in this case comparing 4 with 6 and 5 with 6 means df takes the value of either 2 or 1, respectively).

Defining the growth transition matrix

The data from all sites includes instances of negative increments (Fig. 2) and hence it is not surprising when the predicted increments also feature negative values. This implies that abalone can decrease in size during a time step. However, abalone tend not to exhibit negative growth; instead these negative increments are assumed to be the result of measurement error. The transition probabilities are simply the cumulative normal distribution to the upper size limit of each size class minus the cumulative normal distribution to the lower size limit of each size class in turn:
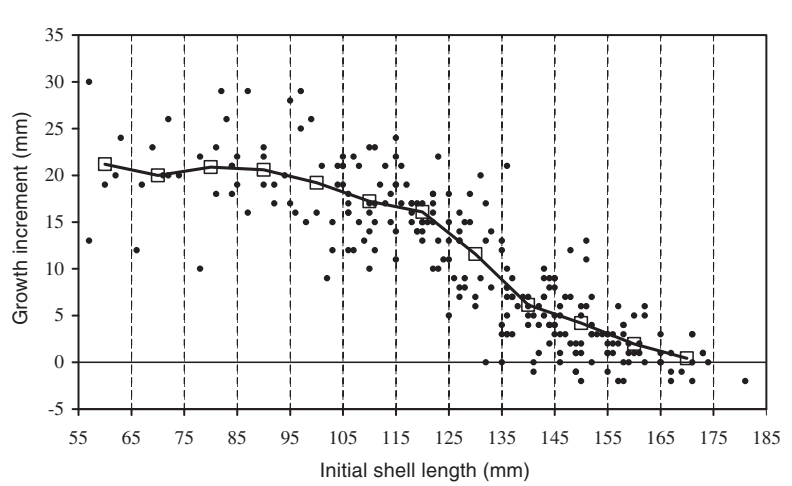
$$G_{i,j} = \int_{-\infty}^{L_i+\frac{LW}{2}} \frac{1}{\sqrt{2\pi}\sigma^j_{L_i}} e^{-\left[\frac{\left(L_i - \bar{L}_{i,j}\right)^2}{2\left(\sigma^j_{L_i}\right)^2}\right]} dL \qquad L_i = L_{Min}$$

$$G_{i,j} = \int_{L_i-\frac{LW}{2}}^{L_i+\frac{LW}{2}} \frac{1}{\sqrt{2\pi}\sigma^j_{L_i}} e^{-\left[\frac{\left(L_i - \bar{L}_{i,j}\right)^2}{2\left(\sigma^j_{L_i}\right)^2}\right]} dL \qquad L_{Min} < L_i < L_{Max}, \quad (10)$$

$$G_{i,j} = \int_{L_i-\frac{LW}{2}}^{+\infty} \frac{1}{\sqrt{2\pi}\sigma^j_{L_i}} e^{-\left[\frac{\left(L_i - \bar{L}_{i,j}\right)^2}{2\left(\sigma^j_{L_i}\right)^2}\right]} dL \qquad L_i = L_{Max}$$

where $G_{i,j}$ = the transition probability of an abalone growing from size class j into size class i;

L_i = the mid-size of size class i;

LW = the size class width; and

Figure 2
Plot of growth increment (mm) after approximately one year against initial length (mm) for blacklip abalone (*Haliotis rubra*) from the southwest region of Tasmania. The vertical dashed lines represent the boundaries of the 10-mm size classes and the curved line and black squares represent the trend and mean growth increments, respectively, for each class of initial sizes. Mean values are only shown for initial size classes representing more than one observation. Negative increments were included in the mean estimates.

σ^j_{Li} = the standard deviation of the normal distribution of growth increments for the initial size class j.

$\bar{L}_{i,j}$ = the expected average final size for initial size class j, which equals $L_j + \Delta\hat{L}_{i,j}$, where $\Delta\hat{L}_{i,j}$ is the average expected growth increment for initial size class j.

Summing the smallest size class to $-\infty$ and the largest size class to $+\infty$ effectively makes both of these size classes plus-groups that ensure that the transition probabilities for all n size classes sum to one.

Length at age

Because of the potentially indeterminate nature of the growth description, there is no analytical version of the growth equation that can provide a length for a given age. Instead, growth needs to be simulated to estimate length at age. That is, an initial length is assumed and then the predicted growth increment in a given time interval (seasonally short or annual) is estimated; this is then added to the initial length and the process is repeated to generate a predicted length at age. The simulated growth increments may include stochasticity (guided by the non-constant variance with initial length) and lead to a scatter of predicted sizes. Alternatively, growth can be simulated by using the growth transition matrix from the model fit. For annual growth only one transition matrix is required, however, to describe seasonal growth there would need to be an array of

growth transition matrices describing the expected growth for different parts of the year.
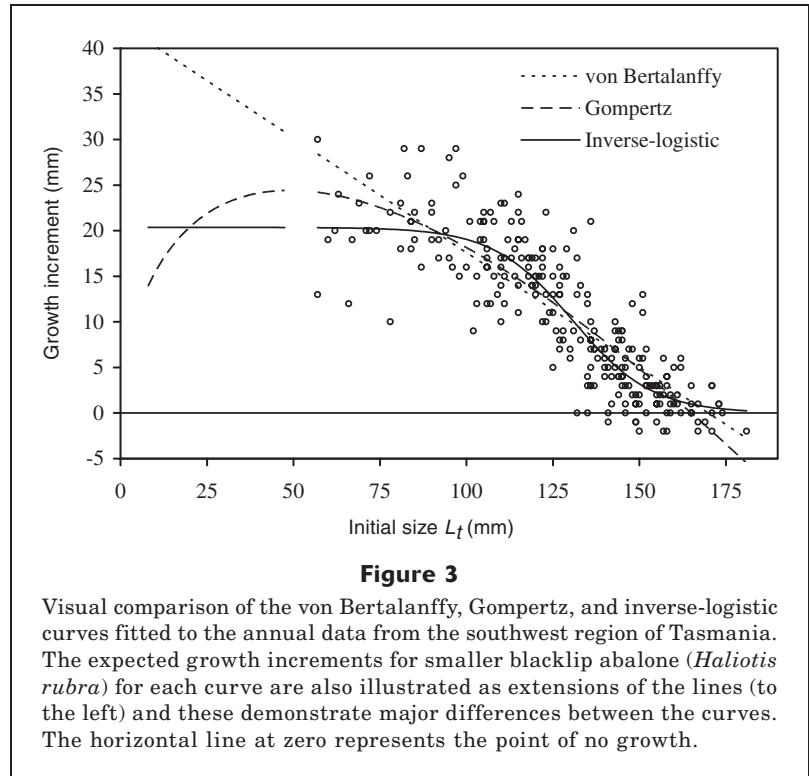
Comparison of productivity between areas

With the inverse-logistic description of growth the parameter combinations do not provide an intuitively obvious indication of the productivity of different areas. A large *MaxΔL* does not necessarily mean an area has high productivity if the large growth increments occur only for relatively small animals. An index of relative productivity can be obtained by applying the growth transition matrix derived for an area to a standard initial vector of numbers at size. The areas considered here were compared by generating an annual transition matrix for each area with 31 five-mm size classes from 60 mm up to 210 mm. This transition matrix was multiplied with an initial numbers-at-size vector containing 1000 individuals in the smallest size class. This multiplication was then repeated iteratively for 10 years of growth (i.e., without mortality). The final numbers at size were converted to mass by using the standard $Weight = aLength^b$ where, in southern Tasmania, a = 5.669E−05 and b = 3.1792, to provide a comparable index of relative productivity between areas in kilograms.
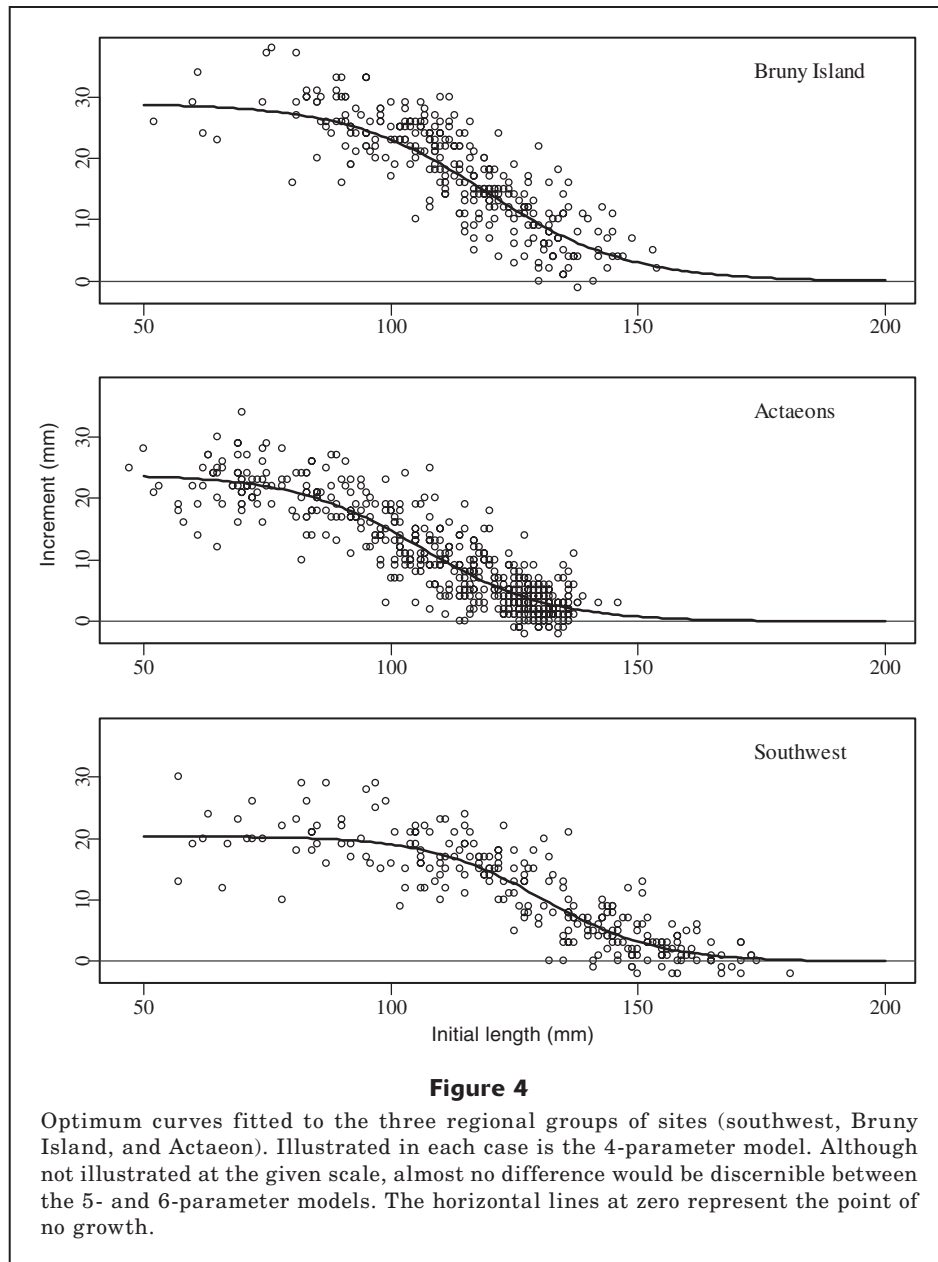

Figure 3

Visual comparison of the von Bertalanffy, Gompertz, and inverse-logistic curves fitted to the annual data from the southwest region of Tasmania. The expected growth increments for smaller blacklip abalone (*Haliotis rubra*) for each curve are also illustrated as extensions of the lines (to the left) and these demonstrate major differences between the curves. The horizontal line at zero represents the point of no growth.

Results

Initial summary of growth patterns

The general growth pattern apparent in the southwest Tasmania (Fig. 2) was also found at other sites around Tasmania, although its full expression was sometimes obscured because the range of available data was limited or truncated by intense size-selective fishing on the larger abalone or because of difficulty in finding cryptic smaller abalone. The growth pattern begins with a relatively constant growth increment (implying linear-like growth) in the smaller-size abalone. This early linear-like growth is followed by a steady decline in growth increment, possibly approaching some minimum annual increment in what would be an asymptotic fashion. Not only do the growth increments follow this decreasing pattern, but a similar pattern is exhibited by the variability of the observed growth increments around the mean trend, although the decrease in variation only occurs at larger sizes (Fig. 2). This pattern of growth differed markedly from the expectation of both the von Bertalanffy and the Gompertz growth models, even when these models were implemented with probability density functions instead of constant parameters (Sainsbury, 1982a; Troynikov et al., 1998; Bardos, 2005).

Instead of these standard curves, the growth pattern observed indicated that some kind of inverse-logistic curve might describe the observations well across the range of available data. If the minimum predicted mean growth increment was greater than zero, it would indicate indeterminate growth in which the dynamics would permit growth to continue (possibly very slowly) until each animal died. An alternative way of looking at indeterminate growth is to note that there may be an upper size limit, at which the growth increment becomes zero, but it is so high that individuals never reach it before death.

Comparison of the inverse-logistic, von Bertalanffy, and Gompertz models

For the southwest region, the three different growth curves all predicted or described the expected growth of blacklip abalone reasonably well . The overlap between the von Bertalanffy and Gompertz curves was especially close over this range (Fig. 3). However, at smaller and larger sizes all three curves diverged significantly. The von Bertalanffy and Gompertz curves both predicted negative growth increments beyond the L_∞ (although using a probabilistic version of these curves could prevent this problem). The major difference between the three curves was therefore found in what was predicted for smaller abalone. The von Bertalanffy curve predicted linearly decreasing growth increments (Fig. 3) as initial size increased. The Gompertz curve predicted initial exponential growth, starting from very small increments

Figure 4

Optimum curves fitted to the three regional groups of sites (southwest, Bruny Island, and Actaeon). Illustrated in each case is the 4-parameter model. Although not illustrated at the given scale, almost no difference would be discernible between the 5- and 6-parameter models. The horizontal lines at zero represent the point of no growth.

for the smallest abalone and reaching a maximum and tailing off as initial length increases. Finally, the inverse-logistic curve predicted constant increments for smaller abalone (initial linear growth) until the growth increments began to decrease with increasing initial length.

The minimum *AIC* and *BIC* were produced by the 4-parameter inverse-logistic curve and not by the 3-parameter von Bertalanffy and Gompertz curves. The log-likelihoods were −726.1 for the von Bertalanffy, −712.2 for the Gompertz, and −681.1 for the inverse-logistic model. With only one more parameter than the other two models, a likelihood ratio test implies that the inverse-logistic curve was a significant improvement over the other two curves.

Annual growth descriptions

Within each of the three regional groups of sites, the predicted mean growth increment for given initial shell lengths for the 4-, 5-, and 6-parameter models was very similar (Fig. 4). In the case of the southwest and Actaeon regions, the predicted lines were visually coincident, whereas for Bruny Island there were only very slight differences in the three curves (Table 2).

For both the southwest and the Actaeon regions, the 4-parameter model was deemed the optimum model configuration by both the AIC and BIC. For the Bruny Island region, the BIC indicated that the 4-parameter model was optimal and the AIC indicated the 6-param-

Table 2

Alternative annual model structures, with their parameters, for the three regional groups of collection sites. The number after each regional name denotes the number of free parameters fitted to the available data. For site locations see Figure 1 and Table 1. $Max\Delta L$ is the hypothetical asymptotic maximum growth increment, L_{50}^m is the initial length at which the midway point between the $Max\Delta L$ and lowest growth increment is reached, and L_{95}^m denotes the initial length at which 95% of the difference between the smallest and maximum increment is reached. $Max\sigma_L$ is the hypothetical asymptotic maximum standard deviation, L_{50}^S and L_{95}^S are the inverse-logistic parameters describing how the variability of residuals decreases with increasing L_t, and Prod Kg is the relative productivity in kilograms derived from the respective transition matrix. See Equations 1 and 2.

Model	$Max\Delta L$	L_{50}^m	L_{95}^m	$Max\sigma_L$	L_{50}^S	L_{95}^S	Prod Kg
Southwest 6	20.393	130.648	164.824	4.461	163.736	214.934	473.5
Southwest 5	20.381	130.669	164.768	4.396	163.735	210	473.1
Southwest 4	20.364	130.688	164.551	4.346	L_{95}^m	210	472.1
Actaeons 6	23.922	106.084	144.431	4.311	138.679	175.809	308.4
Actaeons 5	23.889	106.136	144.243	4.623	142.934	210	308.6
Actaeons 4	23.873	106.165	144.152	4.551	L_{95}^m	210	308.1
Bruny Island 6	28.612	119.736	160.142	4.267	151.438	160.876	459.2
Bruny Island 5	28.386	119.893	159.105	4.297	173.763	210	453.3
Bruny Island 4	28.916	119.421	161.336	4.603	L_{95}^m	210	467.2

Table 3

For each model and parameter combination, the Bayesian information criterion (BIC), Akaike information criterion (AIC), negative log-likelihood (–veLL), and total number of observations n are given. The italicized cells denote the minimum for each criterion and region. The columns labeled "Model 5" and "Model 4" denote the likelihood ratio test values compared to the models in the Model column. The comparisons in Model 5 column had one degree of freedom and for the 5-parameter model to be better than the 4-parameter, it had to be greater than $\chi_1^2 = 3.84$, and the comparisons in the Model 4 column had two degrees of freedom and had to be greater than $\chi_2^2 = 5.99$ for the models with more parameters to be significantly better than the 4-parameter model.
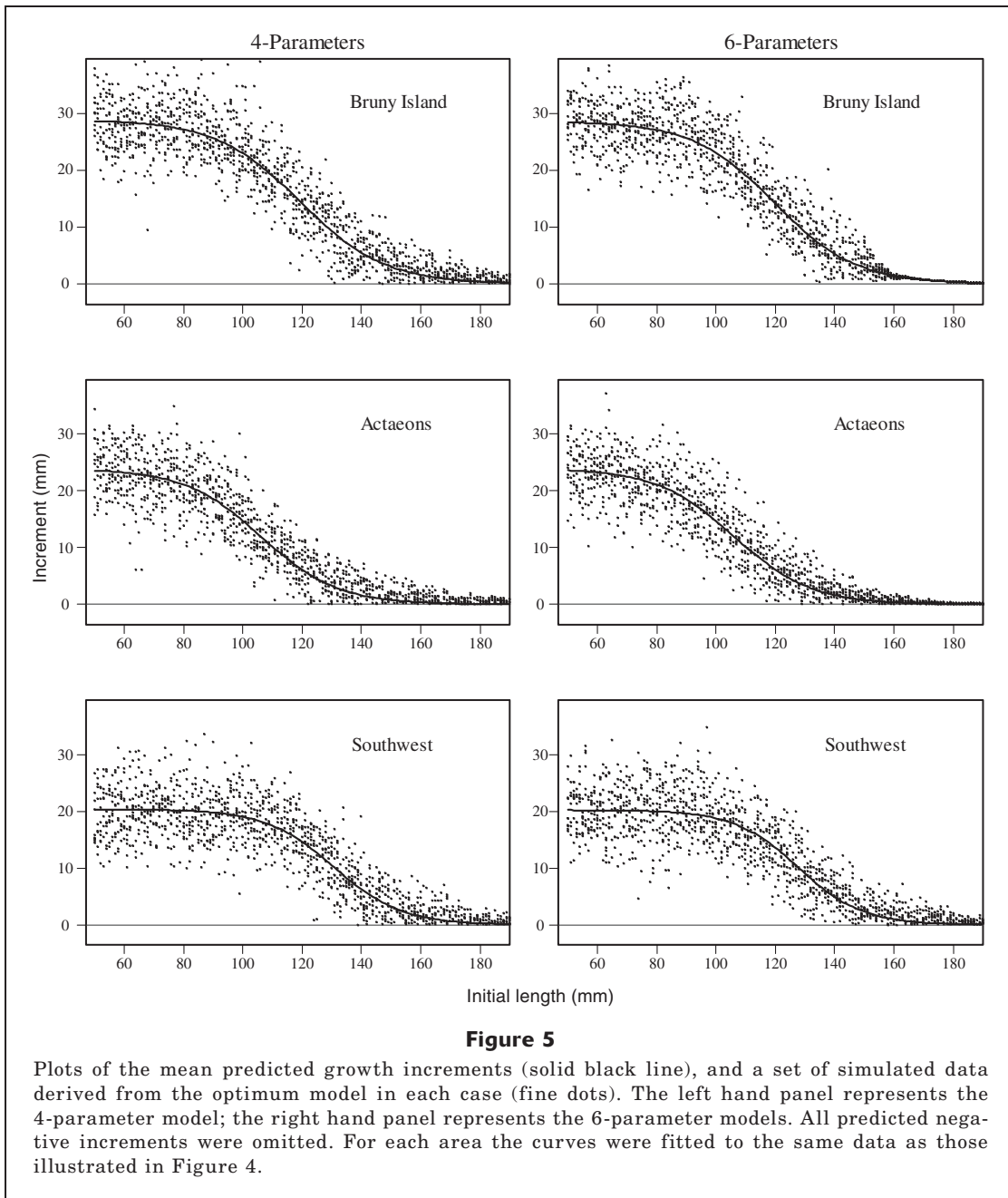
Model	BIC	AIC	-veLL	n	Model 5	Model 4
Southwest 6	1395.1	1373.9	680.96	252	0.14	0.18
Southwest 5	1389.7	1372.1	681.03	252		0.04
Southwest 4	*1384.2*	*1370.1*	681.05	252		
Actaeons 6	2716.3	2690.9	1339.5	500	3.6	3.8
Actaeons 5	2713.7	2692.7	1341.3	500		0.2
Actaeons 4	*2707.6*	*2690.7*	1341.4	500		
Bruny Island 6	1747.6	*1725.5*	856.7	295	2.4	4.8
Bruny Island 5	1744.2	1725.8	857.9	295		2.4
Bruny Island 4	*1740.9*	1726.2	859.1	295		

eter model was optimal (Table 3). At the same time, the likelihood ratio test indicated in all cases that the 4-parameter model was not significantly worse than any other model (Table 3; Fig. 3).

The key differences that occur between the fitted models relate to how well they describe the trends in variation along the curves. The data for the southwest had the widest size range and the similarity of the fitted L_{50}^S parameter to the L_{95}^m parameter was clear. At the same time, the L_{95}^S parameter was only slightly bigger than 210 mm (Table 2). Thus, the substitutions to create the 4-parameter model had little effect on the outcome if this model was used to predict the likely distribution of growth increments (Fig. 5). The main effect of reducing the number of parameters used was to slightly reduce the variation beyond about 170 mm initial shell length.

The 6-parameter model has sufficient flexibility in that it can accurately describe both the mean growth trend and the pattern of variation around the expected mean growth increments. This was not necessarily an advantage when the high level of fishing mortality applied to legal-size abalone means that the availability of larger size abalone in the tag return data can be

Figure 5

Plots of the mean predicted growth increments (solid black line), and a set of simulated data derived from the optimum model in each case (fine dots). The left hand panel represents the 4-parameter model; the right hand panel represents the 6-parameter models. All predicted negative increments were omitted. For each area the curves were fitted to the same data as those illustrated in Figure 4.

limited and only provided a biased perception of the growth of larger abalone. With the southwest data the difference between the 4- and 6-parameter models was slight; however, larger differences were found when the 4- and 6-parameter models were applied to the other two regions, which were less well represented in the larger initial sizes (Fig. 4). Most obviously, at Bruny Island (Fig. 5), the 6-parameter model so closely described the available data that beyond about 160 mm, the model predicted essentially no variation around the predicted mean growth increments. Although the 6-parameter model accurately described the available

data, the 4-parameter model provided a more realistic representation of the spread of predicted growth increments for initial sizes for which there were few or no observed data (Fig. 5).

Of the three regions considered, the southwest and Bruny Island were similar in terms of relative productivity and the Actaeon regional sites were the least productive (Table 2). The parameter combinations for the southwest and Bruny Island regions were rather different, but although the *MaxΔL* was 8 mm larger at Bruny Island than in the southwest, it was offset in the southwest by the higher value for L_{50}^m. The two sites

constituting the Actaeon region samples were within relatively low productivity areas that may be considered to be atypically low for the Actaeon area (see the seasonal analysis).

Table 4

Seasonal growth-description parameter estimates. All parameter definitions are given with Equation 1 under the heading "Growth model" in the Materials and methods section. In the Actaeon Island estimates L_{50}^S and L_{95}^S reached the limits placed on the parameters. At Sterile Island, the parameter estimates obtained did not change when the L_{50}^S and L_{95}^S estimates were replaced with 209 and 210, respectively. In all cases the logistic reduction in the variance was negligible. The –veLL is the negative log-likelihood. Productivity, in kilograms, is the relative productivity derived from the respective transition matrix.

Parameter	Actaeon Island	Sterile Island
$Max\Delta L$	21.8464	20.0111
L_{50}^m	129.9702	121.7953
L_{95}^m	162.1723	161.4016
$Max\sigma_L$	6.7129	6.8766
L_{50}^S	209	186.9362
L_{95}^S	210	192.3000
C	0.1123	0.0907
p	0.1263	0.1561
C_σ	−0.0821	−0.0489
Productivity Kg	484.2	419.4
-veLL	1249.673	944.564
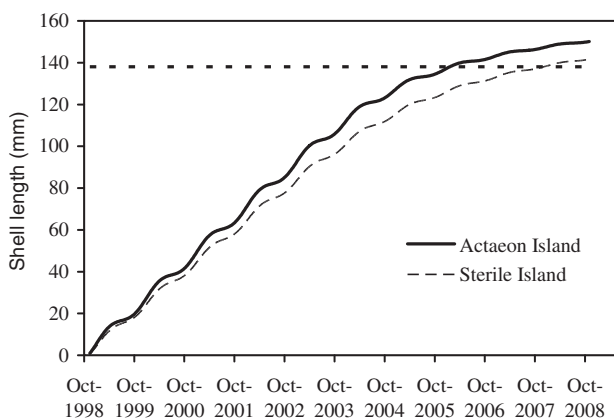
Figure 6

A comparison of the implied seasonal growth curves at the Actaeon and Sterile Islands in southern Tasmania. The fine horizontal dashed line at 138 mm is the current legal minimum length. The curves remain approximately linear until about 100 mm shell length. The slowest growth periods line up approximately with October each year.

Seasonal growth descriptions

Seasonal growth descriptions were fitted to data from two sites in southeast Tasmania: Actaeon Island and Sterile Island (Table 1; Fig. 2). In each case, when the inverse-logistic curve describing the standard deviation of the residual errors was fitted, the estimates of L_{50}^S and L_{95}^S were both much larger than the maximum size observed. In effect, this result implied that the variability was best described with Equation 7 rather than Equation 3. For this reason, the 7-parameter model was preferred to the 9-parameter model, even though the optimum fit in each case lead to the same results in terms of parameter estimates and log-likelihood. The two sites are very close together geographically (~2 km apart) and, in this case, the parameter estimates were similar between the two sites (Table 4).

By assuming a starting size of 0.25 mm on the 25th November (a typical size and date of settlement for a newly settled blacklip abalone) in an arbitrary year, and by calculating the expected size increment in a series of 8-day steps forward in time, adding those increments to the initial size and then repeating the process, it was possible to visualize the seasonal growth of animals (Fig. 6). The main difference in the parameters is in the L_{50}^m, which was 8.0 mm larger at Actaeon Island (Table 4). This difference led to the abalone at Actaeon Island reaching the current minimum legal length of 138 mm in approximately eight years, whereas the difference led to the current minimum legal length in nine years, on average, at Sterile Island (Fig. 6).

The Actaeon Island site was far more productive than Gagens Point and the Middle Ground, both in the Actaeon region and, in fact, was as productive as both the Bruny Island and southwest regions (Tables 2 and 4). The Sterile Island site had a productivity that was only 89% of that of the Actaeon Island site (431 kg vs. 485 kg; Table 4), this was also reflected in a one year difference in time to legal minimum size (Fig. 6).

The pattern of seasonality was very similar between the two sampled sites; linear-like initial growth proceeded at least until 100 mm shell length. The phase parameter, p, value of 0.118 implies that the fastest period of growth occurred on 11th February at the Actaeon Islands, whereas at Sterile Island the estimate of 0.156 indicates the fastest growth occurred two weeks later on 25th February.

Discussion

Comparison of inverse-logistic, von Bertalanffy, and Gompertz models

The major difference between the inverse-logistic growth description, the von Bertalanffy growth curve, and the Gompertz growth curve is seen in the model fit at the extremes of the growth trajectory. Without

a probabilistic interpretation of the parameters, the von Bertalanffy and Gompertz curves predict negative growth increments at initial lengths greater than L_∞, and the inverse-logistic predicts ever decreasing growth increments as the initial length at tagging increases. Thus, a realistic representation of the final size distribution of larger abalone is provided by the inverse-logistic model without the complexity of a probabilistic interpretation of the parameters. In Tasmania, the growth of small abalone, at least above 10 mm, appears to be linear-like and to increase in relatively constant growth increments through time (Prince et al., 1988; Gurney et al., 2005). Although the von Bertalanffy and Gompertz equations can approximate linear-like growth over these small sizes, linear growth limits their capacity to describe accurately the growth of larger animals at the same time. The von Bertalanffy curve predicts a linear relationship between growth increment and initial shell length. The Gompertz equation, on the other hand, predicts that small abalone would have very small growth increments that initially increase with initial length and then decline again. Neither of these alternatives is consistent with observations in Tasmania of linear-like early growth.

Growth pattern

The tagging data on growth increments of blacklip abalone from various sites around the south of Tasmania were able to be grouped according to similarity of growth pattern. All regions exhibited a similar pattern of mean growth increments that were well described by a symmetric inverse-logistic curve.

Negative growth increments observed in the tagging data were not taken to be evidence of negative growth, but were rather taken to be a reflection of measurement or recording errors, a possible chipping of shell edges during collection, or an increased chance of shell erosion in disturbed animals (or a combination of these possibilities). Because of this, when simulating growth, negative increments were not included.

The tagging data were, in some cases, truncated either in the smaller or the larger sizes. The fishing mortality rate on legal-size abalone is high and numbers of animals much larger than the minimum legal length are significantly reduced. In addition, the cryptic nature of undersize abalone means that obtaining representative data across the whole size range can be difficult. It is also possible that the tagging process could influence the subsequent rate of growth. Intuitively, if there were an impact, it would probably be a negative bias on the growth increments that would increase the variation observed (by extending growth into smaller increments).

Despite the limitations of the data, the proposed system of two linked inverse-logistic curves proved capable of fitting and simulating data from three sites in southern Tasmania. The inverse-logistic model was fully capable of producing transition matrices with predicted values across the full range of size classes required (60 mm to 210 mm). The truncation of the available

data by high levels of fishing pressure did have effects, however. Surprisingly, the more complex 6-parameter model did not always provide the most workable description of growth because the fit with six parameters could over-emphasize missing data; that is, the absence of data could influence the fitted curve, especially when the flexibility of the 6-parameter curve was used. It can be argued that the simpler 4-parameter model provides a more useful description of growth because it is less likely to be influenced by peculiarities or limitations of the available data. For example, at the legal minimum size limit (136 mm shell length at the time of data collection), abalone from the Bruny Island region were growing an average of 8 mm per annum (with a range from 2 mm to 15 mm). However, fishing mortality rates at Bruny Island were very high and few legal-size animals remained for long at this site with the result that the tagging growth increment data were sparse above 140 mm. The 6-parameter model describes the specific pattern of growth in the data from Bruny Island, truncating any growth beyond the maximum size available, whereas the 4-parameter model extrapolates the growth pattern beyond the maximum size available in the data and, in this case, provides a much more plausible solution. For stock assessment purposes, the 4-parameter model would be more useful in practice. The symmetry of the inverse-logistic curve enables the 4-parameter model to project the growth dynamics into size classes for which there are few or no samples.

Seasonal growth

The independent samples from Actaeon Island and Sterile Island, which are close together geographically, generated very similar estimates of the timing of the seasonal changes in growth rates. These samples were so similar that the mean curves remained close until the abalone reached about 80 mm shell length. The abalone at Actaeon Island, however, continued growing rapidly for longer than the animals at Sterile Island; therefore these curves diverged. An implication of this difference in productivity is that instead of taking about 8 years to reach the legal minimum length, as at Actaeon Island, it takes 9 years at Sterile Island.

The blacklip abalone at the Middle Ground and Gagens Point sites were selected by local abalone divers as having notoriously slow growth. Compared to Actaeon Island, these two sites in the Actaeon Island region did indeed have relatively low productivity compared to the seasonal sample from Actaeon Island (only about 308 kg relative to 484 kg); and this occurred despite the *MaxΔL* being about 23 mm for the Middle Ground and Gagens Point sites but only 21 mm at Actaeon Island. Productivity was strongly and positively correlated with the L_{50}^m and the L_{95}^m parameter values, which relate to how long the linear-like growth phase continues.

The different sites in the Actaeon region are all relatively close together geographically and yet variation in the parameter estimates and consequent productivity among sites were high. This result is consistent with

the idea that abalone growth is likely to be determined by local site-specific influences in addition to regional scale influences (McShane and Naylor, 1995; Naylor et al., 2006). Thus, although sites within the Actaeon region were variable, similarities were evident between sites located in distant regions (e.g., in the southwest and Bruny Island). This variability in growth has obvious implications for the confidence with which it is possible to conduct stock assessments for abalone over large areas. The description of growth in size-structured models is so influential that the interpretation of any model outputs would need to be made with great attention paid to any potential biases brought about by using an under- or over-productive description of growth.

Estimates of productivity derived from the inverse-logistic description of growth would be expected to lie somewhere between that predicted by the von Bertalanffy curve and the Gompertz curve. The von Bertalanffy curve predicts very rapid early growth and so, all other things being equal, would predict the highest productivity levels, whereas the Gompertz curve predicts very slow early growth and thus would predict the lowest productivity. These differences are why the selection of the most appropriate model of growth is critical for stock assessments. For blacklip abalone in Tasmania the inverse-logistic model provides the most realistic representation of the dynamics of growth.

Acknowledgments

Literature cited

Bardos, D. C.
    2005.   Probabilistic Gompertz model of irreversible growth.   Bull. Math. Biol. 67:529–545.
Breen, P. A., S. W. Kim, and N. L. Andrew.
    2003.   A length-based Bayesian stock assessment model for the New Zealand abalone *Haliotis iris*.   Mar. Freshw. Res. 54:619–634.
Burnham, K. P., and D. R. Anderson.
    2002.   Model selection and multimodel inference: A practical information-theoretic approach, 2nd ed., 488 p.   Springer, New York, NY.
Day, R. W., and A. E. Fleming.
    1992.   The determinants and measurement of abalone growth.   *In* Abalone of the world. Biology, fisheries and culture; proceedings of the 1st international symposium on abalone (S. A. Shepherd, M. J. Tegner, and S. A. Guzman Del Proo, eds.) p. 141–168.   Fishing News Books, Carlton, Victoria, Australia.
Fabens, A. J.
    1965.   Properties and fitting of the von Bertalanffy growth curve.   Growth 29:265–289.

Francis, R. I. C. C.
    1988.   Maximum likelihood estimation of growth and growth variability from tagging data.   NZ. J. Mar. Freshw. Res. 22:42–51.
Francis, R. I. C. C.
    1995.   An alternative mark-recapture analogue of Schnute's growth model.   Fish. Res. 23:93–111.
Gompertz, B.
    1825.   On the nature of the function expressive of the law of human mortality, and on a new model of determining the value of life contingencies.   Philos. Trans. R. Soc. Lond. Ser. B.. Biol. Sci 115:513–585.
Gorfine, H., B. Taylor, M. Cleland, M. Haddon, A. Punt, D. Worthington, and I. Montgomery.
    2005.   Development of a spatially-structured model for stock assessment and TAC decision analysis for Australian abalone fisheries, 42 p.   Fisheries Research and Development Corporation. Primary Industries Research Victoria, Queenscliff, Victoria.
Gurney, L. J., C. Mundy, and M. C. Porteus
    2005.   Determining age and growth of abalone using stable oxygen isotopes: a tool for fisheries management.   Fish. Res. 72:353–360.
Haddon, M.
    2001.   Modelling and quantitative methods in fisheries, 406 p.   CRC Press, Chapman and Hall, Boca Raton, FL.
McShane, P. E., and M. G. Smith.
    1992.   Shell growth checks are unreliable indicators of age of the abalone *Haliotis rubra* (Mollusca, Gastropoda).   Aust. J. Mar. Freshw. Res. 43:1215–1219.
McShane, P. E., and J. R. Naylor.
    1995.   Small-scale spatial variation in growth, size at maturity, and yield- and egg-per-recruit relations in the New Zealand abalone *Haliotis iris*.   NZ. J. Mar. Freshw. Res. 29:603–612.
Naylor, J. R., N. L. Andrews, and S. W. Kim.
    2006.   Demographic variation in the New Zealand abalone *Haliotis iris*.   Mar. Freshw. Res. 57:215–224.
Prince J. D., T. L. Sellers, W. B. Ford, and S. R. Talbot.
    1988.   Recruitment, growth, mortality and population structure in a southern Australian population of *Haliotis rubra* (Mollusca, Gastropoda).   Mar. Biol. 100:75–82.
Punt, A. E., and R. B. Kennedy.
    1997.   Population modelling of Tasmanian rock lobster, *Jasus edwardsii*, resources.   Mar. Freshw. Res. 48: 967–980.
Quinn, T. J., and R. B. Deriso.
    1999.   Quantitative fish dynamics, 542 p.   Oxford Univ. Press, Oxford.
Sainsbury, K. J.
    1982a.   Population dynamics and fishery management of the paua, *Haliotis iris* I. Population structure, growth, reproduction, and mortality.   NZ. J. Mar. Freshw. Res. 16:147–161.
Sainsbury, K. J.
    1982b.   Population dynamics and fishery management of the paua, *Haliotis iris* II. Dynamics and management as examined using a size class population model.   NZ. J. Mar. Freshw. Res. 16:163–173.
Schnute, J.
    1981.   A versatile growth model with statistically stable parameters.   Can. J. Fish. Aquat. Sci. 38:1128–1140.
Sullivan, P. J., L. Han-Lin, and V. F. Gallucci.
    1990.   A catch-at-length analysis that incorporates a

stochastic model of growth. Can. J. Fish. Aquat. Sci. 47:184–198.

Troynikov, V. S., and H. K. Gorfine.
    1998. Alternative approach for establishing legal minimum lengths for abalone based on stochastic growth models for length increment data. J. Shell. Res. 17:827–831.

Troynikov, V. S., R. W. Day, and A. M. Leorke.
    1998. Estimation of seasonal growth parameters using a stochastic Gompertz model for tagging data. J. Shellfish Res. 17:833–838.

von Bertalanffy, L.
    1938. A quantitative theory of organic growth (Inquiries on growth laws. II). Human Biol. 10:181–213.

Worthington, D. C., R. C. Chick, C. Blount, P. A. Brett, and P. T. Gibson.
    1998. A final assessment of the NSW abalone fishery in 1997. Fish. Res. Assess. Ser. 5:1–33.